Automated shotcrete 3D printing - Printing interruption for extended component complexity

Lukas Lachmayer[1], Robin Dörrie[2], Harald Kloft[2], Annika Raatz[1]

[1]Leibniz University Hannover, Germany
[2]Technische Universität Braunschweig, Germany

lachmayer@match.uni-hannover.de, r.doerrie@tu-braunschweig.de

Abstract -

This paper introduces a new approach for extending the geometrical freedom of shotcrete 3D printing. Up to now, manual shotcrete manufacturing and the shotcrete printing process has been performed with a continuous material flow to avoid nozzle clogging, which is caused by the solidification of the fresh material within the printing system. However, this requires a continuous printing path for the entire component, which leads to considerable confines in terms of printable geometries. To overcome this restriction, potential factors to control the printing interruption process were determined and quantitatively investigated. Based on 3D specimen data, the most suitable parameter settings for realizing deterministic short term printing gaps without nozzle blockage were identified. For final validation, these settings served in the robotic fabrication of a test element and showed promising results.

Keywords -

shotcrete 3D printing (SC3DP), concrete construction, robotic fabrication, automation, process control, surface scanning

1 Introduction

The current 3D printing technology ranges from sophisticated and well-developed small-scale 3D printing with various materials [1] up to large-scale printing of steel, recycled materials, and concrete [2, 3, 4]. In particular, the production of constructive concrete components for the construction industry holds the prospect of increasing productivity and efficiency through more targeted use of materials. However, large-scale printing, especially with concrete, is still under development and presents new challenges relating to the fresh concrete characteristics and its handling [5]. One of these challenges is the control and supervision of the material flow during the printing process, caused by two opposing printing requirements. While good flow properties are essential during conveyance of the fresh material, high green strength is necessary immediately after the application to prevent the component from plastic collapse.

To adress this conflict, a novel technique of shotcrete 3D printing (SC3DP) was designed at the Institute of Structural Design (ITE) at the Technische Universität Braunschweig [6]. In this process, the concrete is applied layer-by-layer with high kinetic energy, accelerated by pressurized air. The air flow is mixed into the concrete flow right at the end of the printing nozzle, thus the material is sprayed instead of extruded. Additionally accelerator can be added to decrease the curing time and improve the component stability. This technique is particularly used for the manufacturing of large scale, constructive concrete elements without formwork. In contrast to 3D extruded concrete elements [7], the shotcreted concrete elements obtain a monolithic structure with a much stronger interlayer bond [8]. Consequently the initial risk of plastic collapse is reduced. This behaviour further enables printing of more significant overhangs and also on walls and ceilings.

Despite these advantages, the shotcrete 3D printing process is more susceptible to the risk of nozzle clogging during the printing. This is caused by the necessity of improved flow properties to ensure the sprayability of the material. Hence, the time window between pumpability and solidification must be narrowed to prevent elastic buckling, which will increases the chance of material solidification and nozzle clogging [9]. In this regard, ACI 506R-90 (*Guide to Shotcrete*) requests the material flow to be steady and uninterrupted during manual nozzle operation.

Additionally, the hose length, the pump inertia, and the valve lags avert a step response of the material flow to printing interruption or reactivation commands. For this reason, the temporary stoppage is not only accompanied by clogging [10] and material overrun but also unidentified idle times occur, when restarting the printing process. This clearly demonstrates that printing interruptions lead to reduced component quality.

For standard surface shotcrete manufacturing and basic 3D components, this can be bypassed through a continuous printing path [11]. Nonetheless, while investigating the manufacturing of complex geometries by SC3DP, the path planning becomes more complex as well. As result,

a continuous material flow is not suitable anymore and reduces the geometrical freedom along with increasing the material wastage. Solving this is essential to enter the next stage of geometrical complexity in SC3D printed elements. Thus, it is necessary to control the distribution of the material with an integrated system that determinately starts and stops the concrete flow.

Concerning this matter, the rheological properties and the system inertia are crucial for the deviation between as-planned and as-printed gap. However, in this study we will focus on the system. This given, the concrete valve status, controlling the concrete volume flow, and the pump actuation timing are most important for the inertia. Reasons for this correlation are the hose length and the accumulation of the material within the nozzle. While the hose length results in a severe delay between pump activation and material application, the residual material from the nozzle is distributed even after the valve is shutdown. To counteract this inertial system behaviour, the necessary setting of delay and lead times is identified and optimised in this work.

2 Background and motivation

Looking at state-of-art 3D printing processes, material application interruption is an integral part of all processes. This function is indispensable, especially for the production of complex parts, produced with 3 axis printers and 2.5D path planning algorithms. Thus, multiple methods for the realization of such interruption are available.

2.1 3D printing overview

In small scale Fused deposition (FDM) 3d printing with thermoplasitc or other firm synthetic materials the option of retracting the material from the nozzle was established by changing the rotation of the extruder motor [12]. Hereby the pressure inside the nozzle is decreased and the molten material will not be extruded. A similar approach is used in the small-scale particle bed printing, where the adhesion substance is retracted from or not pumped further into the nozzle. In the process of large-scale concrete deposition, these solutions of material retraction are no longer feasible. Due to long pumping distances and time-dependent material processing the distribution can only be interrupted for a certain amount of time. In the case of contour crafting [13] and concrete extrusion it is possible to release the pressure from the end effector and the pumping system or use trowels to stop the concrete flow. Moreover, the material properties enable the idle mode of the concrete and let it stay inside the nozzle. However, this process becomes more complex when the material is deposited with a certain nozzle distance and additionally accelerated, such as in SC3DP.

2.2 SC3DP

The SC3DP Process was invented in the 1920s and is now being rediscovered as an additive manufacturing technique used in combination with precise robotic fabrication [14]. Through this combination it is possible to manufacture constructive concrete elements without formwork and with integrated reinforcement [4, 6]. The shotcrete 3D printing system used for our research is part of the Digital Building Fabrication Laboratory (DBFL) at the ITE. [15] In this setup a Stäubli TX 200 robot with 6 degrees of freedom is attached to a 3-axis gantry portal, provided by OMAG SpA. These are used in combination to carry the end effector, which is designed to mix the fresh concrete, the accelerator and the pressurized air. The concrete production and conveying line, which deliver the material towards the end effector, consist of a WM-Jetmix 125 Mixer by Werner Mader GmbH and a WM-Variojet FU Pump. The hose length between the pump and the end effector can be up to 25 m for large scale printing. The spray process itself is presented in figure 1. The material used for the printing of all components is a fibre reinforced plain cement concrete produced by MC Bauchemie Müller.

The control system of the entire plant consists of three sub-units. The major control is carried out via G-Code commands on a Siemens sinumerik 840D. For positioning, nine motion commands are mandatory, consisting of three parameters for the gantry portal and six values for the robot. The movement commands for the three-axis gantry are processed directly on the Siemens Sinumerik, while the motion commands for the robot are transferred to the Stäubli control unit.
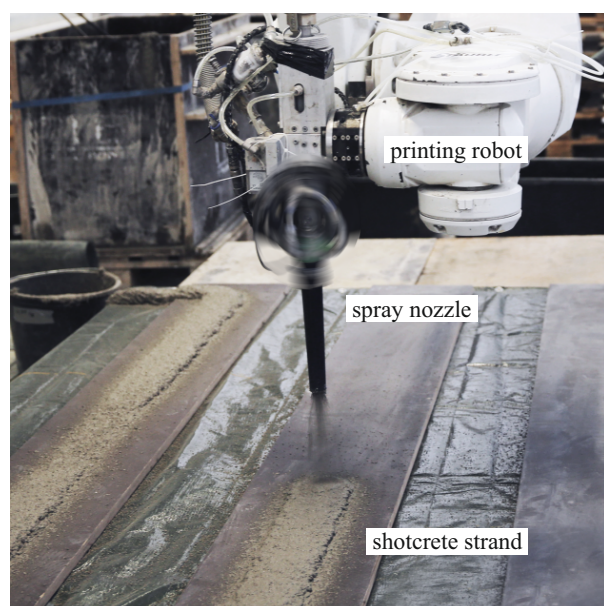

Figure 1. Specimen production by SC3DP

For the control of the concrete, air and accelerator volume flows, G-code commands are forwarded to a Beckhoff industrial PC. To date, these commands are set in the beginning of each printing file and are not changed during the printing process. However, for realization of printing interruption it is necessary to interact with the concrete pump and the concrete valve while printing.

Considering the presented set-up, a wide range of process parameters can be identified which influence the material application. On the one hand, nozzle distance, nozzle diameter, printing speed and spray orientation will directly influence the strand geometry. On the other hand, concrete and air volume flow will suffer a delay due to the mentioned system inertia, before affecting the strand properties. Regarding the aimed printing interruption, the concrete flow will have a major influence on the applied material. Thus, the pump's on and off time, as well as the concrete valve timing are the main parameters for our research.

3 Experimental setup

To investigate the pump and valve timing in consideration of the applied material and possible clogging risks, our first experiment intends to achieve a printing gap with a defined start and endpoint. Another focus lies on the strand geometry itself, thus the investigation also focuses on the restoration of the initially intended path height and width. The amount of material at the set start and end point indicate the change of this geometry. For additional validation of the final parameter setting, a more complex structural element is chosen. The proposed column capital in figure 6 generates a printing path with multiple gaps and will confirm the integration in the existing control system.

3.1 Parameter settings

We choose the experimental setup for the delay and lead time investigations according to figure 2. The selected example distance of 500 mm serves as a basis for all short-term interruptions that do not result in any significant material hardening within the printing nozzle. While aiming for a suitable parameter setting to bridge the illustrated printing interruption, the strand height at the shutdown and restart points x_{stop} and x_{start} must not deviate from the average values prior to the interruption. Additionally, the amount of material within the printed gap should be minimized through the correct parameters.

Four operating points are available within the experimental setup to control the concrete pump and the pinch valve. In this regard, $t_{pv,close}$ and $t_{cp,close}$ mark the shutdown points. Since closing the valve interrupts the concrete volume flow $\dot{V}_{con}$ independently of the concrete pump status and excess pressure must be avoided, de-coupling the two actions from each other is not sensible. Therefore, the shutdown commands are combined into Δt_{stop}, which describes the delay between the shutdown process and the arrival at the targeted printing interruption x_{stop}.

In contrast to the shutdown process, a separation of the start-up process makes sense in that the pump must first build up the concrete pressure inside the hose before the material is conveyed through the nozzle. Thus, the start-up timing of the pump $t_{cp,start}$ and the timing of the pinch valve opening $t_{pv,open}$ are set separately within the test plan. Referring to this, $\Delta t_{cp,start}$ and $\Delta t_{pv,open}$ indicate the delay to the targeted restart x_{start}.

According to design of experiment standards we chose a three level design for the two restart factors $\Delta t_{cp,start}$ and $\Delta t_{pv,open}$. Due to the machine workspace we had to omit the central point, so no non-linear relations can be obtained. Since only one parameter is required for the shutdown process, repeat tests were carried out during our investigation. The detailed parameter settings are shown in table 1. For all tests, the nozzle feed rate, which is equivalent to the printing speed, N_{feed} was set to 4.500 mm/min, the concrete volume flow was kept at 0.4 m/h and the pressurized air ran at 30 Nm/h during the printing operation.

3.2 Software implementation

Looking at potential implementations of the interruption mechanism into the printing system, it is necessary to mention the holistic approach that is used for the printing process of concrete elements at the ITE. Here, complex printing paths are programmed using the programming interface Grasshopper for Rhinoceros3d in combination with "Robots" (a plugin developed by the Bartlett School of Architecture). This combination translates a designed geometry intuitively into G-Code which will run the printing system and serves to visualize the process control for robotic fabrication. Therefore, the identified feed forward times and printing interruption commands must be implementable into G-Code for use during the robotic fabrication process.

Hence the time offset primarily determines the interrelation between the applied material, and the pump and valve actuation, the settings for Δt_{stop}, $\Delta t_{cp,start}$ and $\Delta t_{pv,open}$ are specified in ms as can be found in table 1. However, due to the sequential processing of the G-Code, no time-based output of command signals is feasible. Thus, the time intervals were changed into travelling distances Δx taking into account the nozzle feed rate. Based on these distances, additional path points were included in the printing path, which serve as trigger points for the pump and valve actuation. Due to the sequential processing of G-code, the pump and valve commands must not be implemented di-
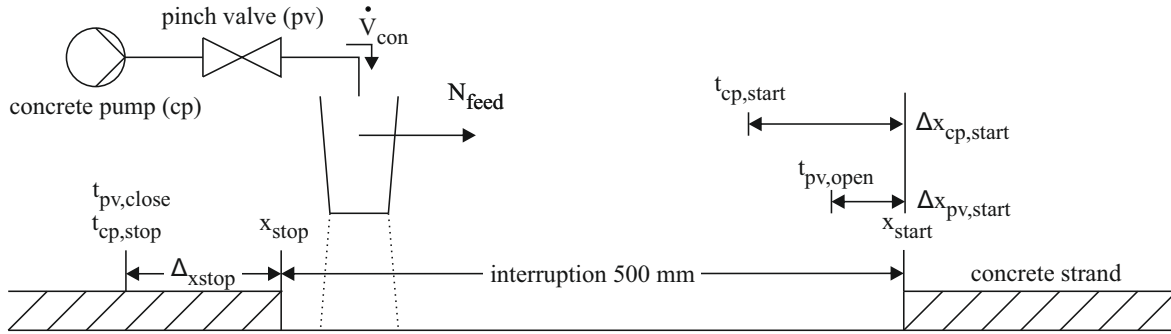
Figure 2. Test setup for investigating the process interruption

Table 1. Investigated process parameter settings

	Δt_{stop}(ms)	Δx_{stop}(mm)	$\Delta t_{cp,start}$(ms)	$\Delta x_{cp,start}$(mm)	$\Delta t_{pv,open}$(ms)	$\Delta x_{pv,open}$(mm)
V1	250	18.75	0	0	0	0
V2	250	18.75	0	0	250	18.75
V3	500	37.50	0	0	500	37.50
V4	500	37.50	1000	75.00	0	0
V5	750	56.25	1000	75.00	500	37.50
V6	750	56.25	2000	150.00	0	0
V7	1000	75.00	2000	150.00	250	18.75
V8	1000	75.00	2000	150.00	500	37.50

rectly as this will cause feed rate interruptions and results in an inconstant material application. Therefore user defined marcos (UMACs) are implemented in the header of each printing files. So, when passing the respective trigger points during the printing process, the specified UMACs were executed to actuate the pump and valve commands. This process is providing a constant nozzle speed and an improved material application while printing.

3.3 Printing path

In order to ensure uniform ambient conditions throughout the investigation and to minimise the influence of external factors on the concrete volume flow, all parameter settings were merged into one single printing path. The complete path is shown in figure 2a). The specimen length was set to 2.200 *mm* in total to ensure volume flow retrieval after the interruptions. It should be noted that the change of the printing direction does not influence the result due to the circular nozzle geometry. This means that the results from linear tests can be transferred to more complex cornering.

3.4 Data evaluation

Changing the selected parameters directly impacts the as-printed gap. This can be obtained by visual inspec-

tion of the specimens presented in figure 3b) and c. For a significant comparison of the process parameters and their influence regarding the interruption, each probe was scanned with a 2D-Laser scanner (Keyence LJ-X8400). Matching the scanner feed rate to the printing speed of 4.500 mm/min while setting the scanning frequency to 10 *Hz* resulted in an evaluation every 7.5 *mm*. Figure 3c) presents an example of the processed measurement data set from V1. Within the scan data, the start and endpoints of the specimens were defined based on strand centre points of the transition regions. The specified transition regions are shown in figure 2b) and are defined by the printed material between to specimens. Both points allowed further identification of x_{stop} and x_{start} in the scans. For subsequent evaluation, the data sets were levelled to the printing surface and the width was set to 200 *mm*. Thus, all data sets contain the same amount of data points.

As marked in figure 3c) the raw 3D data sets were then separated into four areas, each 200 mm in length. The pre and post stop areas were placed around the desired printing shutdown x_{stop} and were used to evaluate the usability of the Δt_{stop} values. Analogously, the pre- and post-start areas surrounding x_{start} were used to evaluate $\Delta t_{pv,open}$ and $\Delta t_{cp,start}$. The purpose of this subdivision was to analyse the amount of the deposited material. Given the initial demands of producing the gap as planned, low

a) printing path
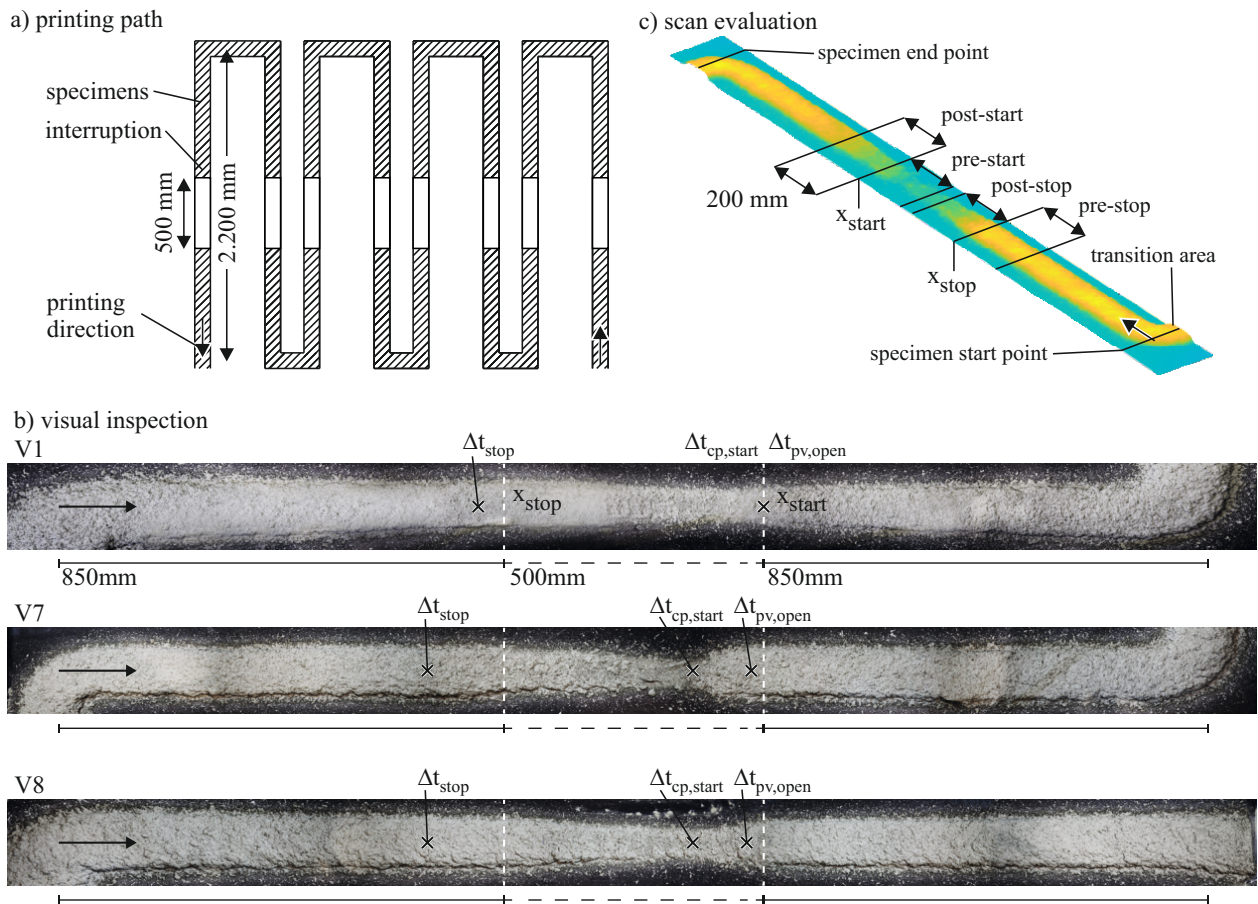
c) scan evaluation

b) visual inspection

Figure 3. a) Printing path setup b) visual inspection and c) scan evaluation of the specimens

quantities of material in the post-stop and pre-start area are to be assessed as positive and low quantities in the other areas as negative. For a quantitative examination, the measured z-values in each area were accumulated. Since the scanned surfaces and the amount of data points are identical for each specimen, the comparison of the accumulated Z-values corresponds to the comparison of the amount of material. Thus, no additional volume calculation is required. The results of the height data evaluation can be seen in figure 4.

4 Results

Since the parameter settings for the investigation of Δt_{stop} were each examined twice, they were summarised for the evaluation. Figure 4a) and b) therefore show only four measuring points, each of which reflects the average value of the two specimens.

Specific evaluation of the pre-stop area in figure 4a) presents an almost constant value across all parameter settings. This confirms the constant material volume flow during the sample production. Therefore, further changes within the recorded data can be attributed to the effects of

the start-up and shutdown processes. Besides, the accumulated height value of $10^5\,mm$ defines the target value for the post-start area.

There is no effect of the closed pinch valve on the applied material volume within the pre-stop area up to $1.000\,ms$ lead time for Δt_{stop}. Source of this seems residual material within the nozzle, which is located on the application side of the valve and is still applied after the valve is closed.

In contrast, the accumulated height in the post stop area displays a decrease of 27 % when raising the pinch valve lead time Δt_{stop} up to $1.000\,ms$. Consequently, closing the pinch valve before reaching the planned printing interruption demonstrates an option to counteract the system's inertia and refrain the material from filling the gap.

Figure 4c) illustrates the results of the evaluation of the pre-start area concerning the valve reopening and the concrete pump restart. In line with the expectations, increasing the valve lead time $\Delta t_{pv,open}$ tends to raise the applied material. Since this is deposited within the printing gap, only low valve lead times for $\Delta t_{pv,open}$ can be recommended initially.

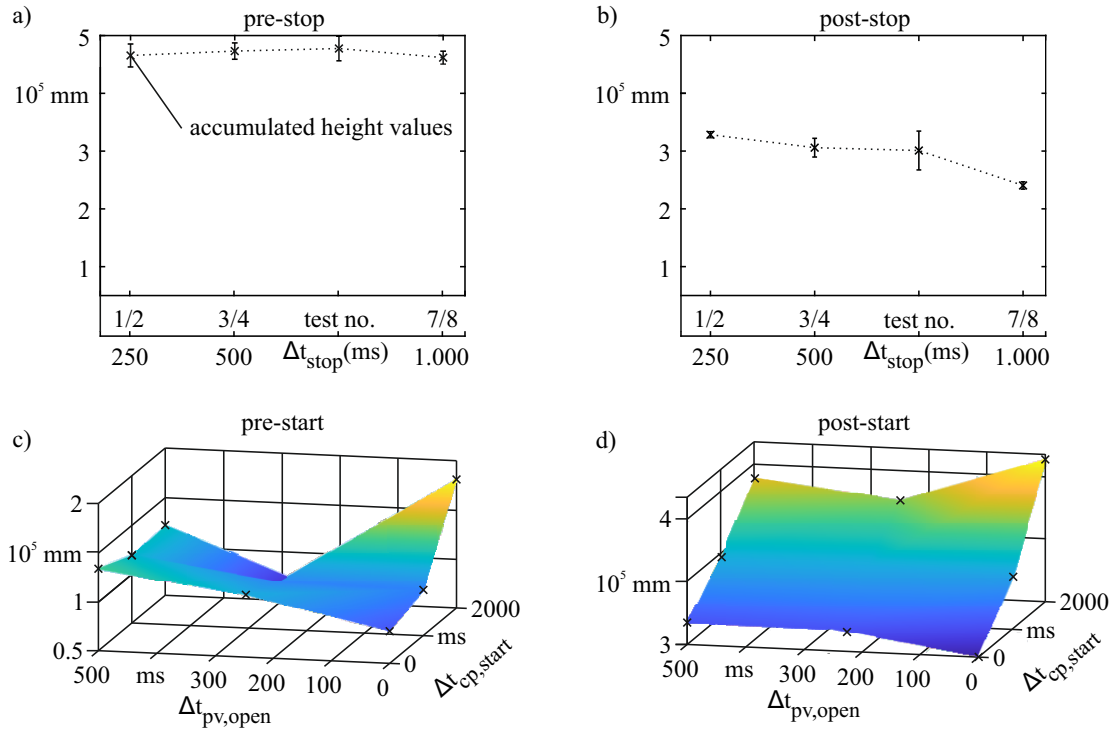It should be noted that when low valve lead times are

Figure 4. Accumulated height values of the scanned sample for evaluation of the sectional material quantity

combined with high pump lead times, which can be observed especially with the combination of $\Delta t_{cp,start}$ 2.000 ms and $\Delta t_{pv,open}$ 0 ms, the highest amount of material is deposited within the gap. This is due to the higher concrete pressure, which increases the material exit velocity after the valve opening resulting in a higher impact. This causes the material to shear and consequently flow into the undesirable pre-start area. Thus, lower valve lead times are unsuitable for the highest concrete pump lead time.

However, taking further into account the post start area, as presented in 4d), an increased pump lead time fosters the material quantity measured after the printing restart. This in turn leads to high contour accuracy after resuming the printing process and thus to a higher component quality.

Given the original requirement for an exact printing of the planned printing interruption, choosing a suitable value for Δt_{stop} is quite evident at 1.000 ms. However, for $\Delta t_{cp,start}$ and $\Delta t_{pv,open}$ the quotient formation according to equation 1 is necessary to determine an optimum in the opposing influences of the factors.

$$\zeta = \frac{post\ start\ [10^3 mm]}{pre\ start\ [10^3 mm]} \quad (1)$$

Hence, this will show a peak for minimal material in the pre-start and maximal material in the post start area. The resulting ratios are shown in figure 5. An optimal
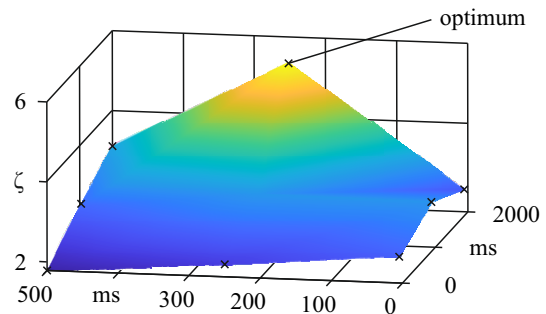

Figure 5. Quotient of pre and post stop area

parameter setting is revealed at a pump lead time of 2.000 ms, and a valve lead time of 250 ms.

In addition, a first test of the presented approach to produce a more complex geometry was performed. A simplified column capital was manufactured to test the print interruption parameters including the automated concrete distribution. The produced component is presented in figure 6. This geometry is composed of eight strands which are combined in the center. The printing process for each layer started on the outer edge and was printed towards the center. The first 15 layers were printed horizontally

Figure 6. Column capital printed with printing interruption routine

and were the basis for the angled layers. The following layers were printed in a 30° angle to produce an overhang on the outside and to orient the layers perpendicular to the assumed force flow in the capital. Using the proposed coding it was possible to design the path planning without overlays or double printed layers. Although the overall quality of the printed geometry shows that printing interruptions are possible, post production process are still necessary to remove the lateral material overhang between the walls. The slight amount of excess material was distributed on the sides of each strand during the reorientation and dry phase of the endeffector due to material overrun. The most obvious solution to avoid this effect is to further delay the stopping time. It should be noted, however, that the increase will also causes the associated Δx_{stop} to rise further. This in return reduces the pump run time which, for short printing paths, may result in a stall of the concrete volume flow. Thus columns, beams and walls will serve as geometries for subsequent tests to analyse the minimal required path length. Given the minimum distance, additional research will focus on up-scaling and defining the maximal interruption time to consider both limits during the path planning of large-scale components.

5 Conclusion

This paper shows a method for realising and optimising short-term printing interruptions during SC3DP. Based on a systematic study, the effect of the systems' inertia could be reduced by implementing lead times for the pump and valve actuation, while avoiding nozzle clogging during the printing. Particularly 1.000 ms were embedded for the shutdown process Δt_{stop}, and 2.000 ms and 250 ms for the restart process of Δcp_{start} and Δpv_{open}. A summary is given in 2.

While decreasing the material overrun by 27 %, the quantity directly after the interruption was increased by 25%. Although printing material is found in the acutal gap,

Table 2. Optimal process parameter settings

Δt_{stop}(ms)	Δx_{stop}(ms)	$\Delta t_{cp,start}$(ms)
1.000	250	18.75

this clearly shows the influence of the chosen parameters and their potential to precisely control the interruption. In particular, the position of the start and end point, as well as the shape of the resulting gap can be improved.

Evidently performing printing interruptions with SC3DP is possible and the precise application decreased the material wastage and expands the path planning possibilities for future components. For further reduction of material overrun, additional tests with increased lead times and printing idle times are scheduled.

6 Acknowledgements

References

[1] Dimitar Dimitrov, Kristiaan Schreve, and Neal de Beer. Advances in three dimensional printing–state of the art and future perspectives. *Rapid Prototyping Journal*, 2006.

[2] Behrokh Khoshnevis. Automated construction by contour crafting—related robotics and information technologies. *Automation in construction*, 13:5–19, 2004.

[3] Tiago A Rodrigues, V Duarte, RM Miranda, Telmo G Santos, and JP Oliveira. Current status and perspectives on wire and arc additive manufacturing (waam). *Materials*, 12:1121, 2019.

[4] Norman Hack and Harald Kloft. Shotcrete 3d printing technology for the fabrication of slender fully reinforced freeform concrete elements with high surface quality: A real-scale demonstrator. In *RILEM International Conference on Concrete and Digital Fabrication*, pages 1128–1137. Springer, 2020.

[5] Hamad Al Jassmi, Fady Al Najjar, and Abdel-Hamid Ismail Mourad. Large-scale 3d printing: the way forward. In *IOP Conference Series: Materials Science and Engineering*, volume 324, page 012088. IOP Publishing, 2018.

[6] H Lindemann, R Gerbers, S Ibrahim, F Dietrich, E Herrmann, K Dröder, A Raatz, and H Kloft. Development of a shotcrete 3d-printing (sc3dp) technology for additive manufacturing of reinforced freeform concrete structures. In *RILEM International Conference on Concrete and Digital Fabrication*, pages 287–298. Springer, 2018.

[7] T Pan, Y Jiang, H He, Y Wang, and K Yin. Effect of structural build-up on interlayer bond strength of 3d printed cement mortars. materials 2021, 14, 236. 2021.

[8] Harald Kloft, Hans-Werner Krauss, Norman Hack, Eric Herrmann, Stefan Neudecker, Patrick A Varady, and Dirk Lowke. Influence of process parameters on the interlayer bond strength of concrete elements additive manufactured by shotcrete 3d printing (sc3dp). *Cement and Concrete Research*, 134:106078, 2020.

[9] Jean-Daniel Lemay, Marc Jolin, and Richard Gagné. Ultra rapid strength development in dry-mix shotcrete for ultra rapid support in challenging mining conditions. In *Proceedings of the Seventh International Conference on Deep and High Stress Mining*, pages 271–279. Australian Centre for Geomechanics, 2014.

[10] Jun Ho Jo, Byung Wan Jo, Woohyun Cho, and Jung-Hoon Kim. Development of a 3d printer for concrete structures: laboratory testing of cementitious materials. *International Journal of Concrete Structures and Materials*, 14:1–11, 2020.

[11] Yuan Jin, Yong He, Guoqiang Fu, Aibing Zhang, and Jianke Du. A non-retraction path planning approach for extrusion-based additive manufacturing. *Robotics and Computer-Integrated Manufacturing*, 48:132–144, 2017.

[12] Md Hazrat Ali, Nazim Mir-Nasiri, and Wai Lun Ko. Multi-nozzle extrusion system for 3d printer and its control mechanism. *The International Journal of Advanced Manufacturing Technology*, 86:999–1010, 2016.

[13] Behrokh Khoshnevis and Dooil Hwang. Contour crafting. In *Rapid Prototyping*, pages 221–251. Springer, 2006.

[14] Joscha Ott, Stefan Neudecker, Jörg Petri, and Harald Kloft. Generative concrete spraying of a freeform chair–a case study. In *Proceedings of IASS Annual Symposia*, volume 2015, pages 1–9. International Association for Shell and Spatial Structures (IASS), 2015.

[15] E Herrmann, JLC Mainka, H Lindemann, F Wirth, and H Kloft. Digitally fabricated innovative concrete structures. In *ISARC. Proceedings of the International Symposium on Automation and Robotics in Construction*, volume 35, pages 1–8. IAARC Publications, 2018.